

# Mesogenic Pyrazaboles: Synthesis, Properties, and Structural Characterization

Joaquín Barberá, Raquel Giménez, and José Luis Serrano\*

*Departamento de Química Orgánica, Facultad de Ciencias-Instituto de Ciencia de Materiales de Aragón, Universidad de Zaragoza-Consejo Superior de Investigaciones Científicas, 50009 Zaragoza, Spain*

*Received August 9, 1999. Revised Manuscript Received October 28, 1999*

A series of disklike compounds containing the pyrazabole ring have been prepared by reaction of 3,5-diarylpyrazoles and borane. The aryl groups are benzene rings substituted with one, two, or three hexyloxy, decyloxy, or tetradecyloxy groups. The study of the liquid crystalline properties shows that the optimal chain length to generate mesomorphism in this family of compounds is 10 carbon atoms. Thus, three compounds with decyloxy substituents show hexagonal columnar mesophases at relatively low temperatures. For two of them bearing 10 and 12 decyloxy chains the mesophase remains stable at room temperature for long periods of time, as confirmed by X-ray diffraction. The crystal structure of the nonmesogenic homologue 1,3,5,7-tetrakis(4'-methoxyphenyl)pyrazabole has been determined by X-ray diffraction. The structure analysis reveals that the pyrazabole cycle adopts a slightly twisted boat conformation. In the crystal packing its molecules stack in columns, which is consistent with the fact that the homologous compounds with long chains generate columnar mesophases.

## Introduction

A few years ago we reported columnar liquid crystal phases in a novel series of mesogenic molecules based on the pyrazabole ring.<sup>1</sup> The basic idea of this work was to use simple organic molecules as subunits and metal or metalloid atoms as links to generate molecules with an appropriate geometry which favors columnar stacking. Within this context, several series of metallo-mesogenic compounds derived from  $\beta$ -diketone have been reported in the literature containing metals as Cu, Ni, Pd, V, Tl, Fe, Mn, Cr, Rh, and Ir.<sup>2</sup> However, apart from our above-cited paper<sup>1</sup> reporting boron-containing derivatives of pyrazole and more recent papers in which we describe the columnar mesomorphism of trinuclear gold(I) complexes derived from the same kind of ligand,<sup>3</sup> no other examples have been reported in derivatives of pyrazole. The planned strategy is to put together two half-disk-shaped promesogenic units through stable bonds with the aim of generating a disklike structure. Initially uncomplexed pyrazoles substituted with several aliphatic chains were investigated as potential discotics by their ability to dimerize through intermolecular hydrogen bonding. However, this objective failed,<sup>4</sup> and

for this reason, we decided to force dimerization by means of covalent bonds using bridging groups such as  $\text{BH}_2$ . In this paper, we have extended our previous study of the first examples of mesogenic pyrazaboles to new members of the series, where we have changed the number and the length of the side chains and their positions in the benzene rings. These molecules, as most of the discotic mesogens, consist of two parts (Table 1):

a rigid central core, formed by the pyrazabole cycle substituted in positions 1, 3, 5, and 7 with benzene rings; and a peripheral flexible region, formed by several alkoxy chains, from a minimum of 4 to a maximum of 12. We prepared a number of 1,3,5,7-tetraphenylpyrazaboles substituted with one, two, or three alkoxy groups (alkoxy = *n*-hexyloxy, *n*-decyloxy, or *n*-tetradecyloxy) on each phenyl ring.

In the design of discotic liquid crystals, the central core of the molecule should preferably be approximately flat. This favors their stacking to generate columnar structures. Single-crystal X-ray analysis of several boron-substituted pyrazaboles (containing  $\text{BR}_2$  bridges,  $\text{R} = \text{Cl}, \text{Br}, \text{CH}_3, \text{SCH}_3$ , etc.) show that the central  $\text{B}_2\text{N}_4$  ring can adopt a chair, boat, or flat conformation depending on the substituents on the boron atom<sup>5</sup> (Figure 1). Unfortunately, there are no data on pyrazaboles containing  $\text{BH}_2$  bridges. If the  $\text{B}_2\text{N}_4$  ring has a chair or a flat structure, then the two pyrazole rings ( $\text{C}_3\text{N}_2$ ) should be coplanar and the whole system should be approximately flat. On the other hand, if the  $\text{B}_2\text{N}_4$  ring adopts a boat conformation, then the pyrazabole is not flat. However, in some cases the absence of planarity in the central core does not preclude columnar

\* To whom correspondence should be addressed. E-mail: joseluis@posta.unizar.es.

(1) Barberá, J.; Giménez, R.; Serrano, J. L. *Adv. Mater.* **1994**, *6*, 470.

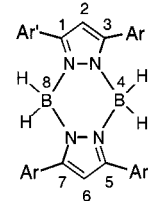
(2) (a) Barberá, J. In *Metallomesogens. Synthesis, Properties and Applications*; Serrano, J. L., Ed.; VCH: Weinheim, 1996; Chapter 4. (b) Trzaska, S. T.; Swager, T. M. *Chem. Mater.* **1998**, *10*, 438.

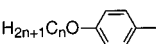
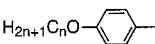
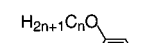
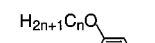
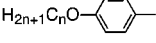
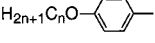
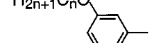
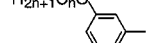
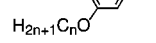
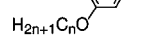
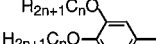
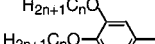
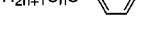
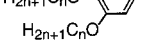
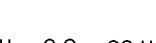
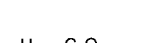
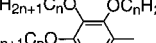
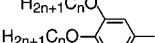
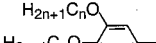
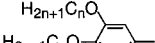
(3) (a) Barberá, J.; Elduque, A.; Giménez, R.; Oro, L. A.; Serrano, J. L. *Angew. Chem., Int. Ed. Engl.* **1996**, *35*, 2832. (b) Barberá, J.; Elduque, A.; Giménez, R.; Lahoz, F. J.; López, J. A.; Oro, L. A.; Serrano, J. L. *Inorg. Chem.* **1998**, *37*, 2960.

(4) Barberá, J.; Catiuela, C.; Serrano, J. L.; Zurbano, M. M. *Liq. Cryst.* **1992**, *11*, 887.

(5) Niedenzu, K.; Noth, H. *Chem. Ber.* **1983**, *116*, 1132.

Table 1. Compounds Prepared and Identification Codes



Compound	number of peripheral chains	chain length n	Substitution on phenyl rings	Ar	Ar'
4C <sub>10</sub>	4	10	4 and 4'		
8C <sub>6-3,4</sub>	8	6			
8C <sub>10-3,4</sub>	8	10	3,4 and 3',4'		
8C <sub>14-3,4</sub>	8	14			
8C <sub>10-3,5</sub>	8	10	3,5 and 3',5'		
10C <sub>6</sub>	10	6			
10C <sub>10</sub>	10	10	3,4 and 3',4',5'		
10C <sub>14</sub>	10	14			
12C <sub>10</sub> unsym	12	10	2,3,4 and 3',4',5'		
12C <sub>10</sub> sym	12	10	3,4,5 and 3',4',5'		

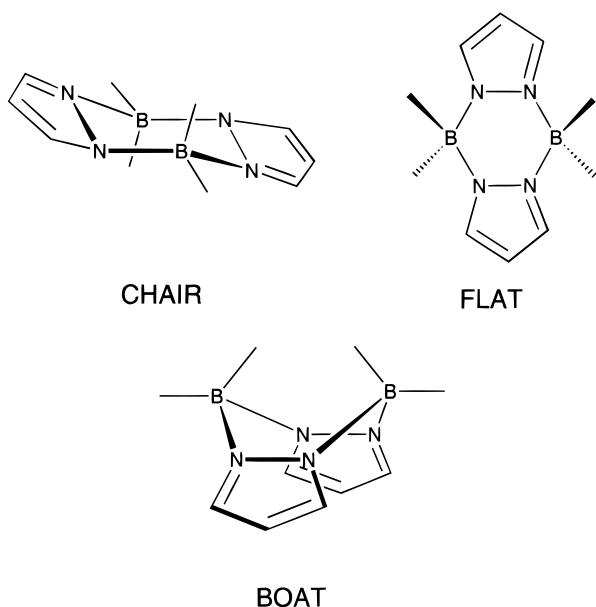


Figure 1. Conformations of the pyrazabole ring.

mesomorphism, as discotics with a wide variety of nonflat shapes have been reported in the literature, which have been called lantern-like,<sup>6</sup> pyramidal,<sup>7</sup> conical,<sup>8</sup> bowl-like,<sup>9</sup> and octahedral.<sup>10</sup> To clarify the geom-

etry of our molecules, a single-crystal X-ray diffraction study was planned. However, all attempts to obtain single crystals of the compounds in the series failed, so we decided to carry out the X-ray study of a model compound, easier to crystallize, that possesses the same central core of tetraphenylpyrazabole and bears only methoxy groups as substituents: 1,3,5,7-tetrakis(4'-methoxyphenyl)pyrazabole.

(6) (a) Giroud-Godquin, A. M.; Marchon, J. C.; Guillon, D.; Skoulios, A. *J. Phys. Lett. (Paris)* **1984**, *45*, 681. (b) Giroud-Godquin, A. M.; Marchon, J. C.; Guillon, D.; Skoulios, A. *J. Phys. Chem.* **1986**, *90*, 5502. (c) Abied, H.; Guillon, D.; Skoulios, A.; Giroud-Godquin, A. M.; Marchon, J. C. *Liq. Cryst.* **1987**, *2*, 269. (d) Maldivi, P.; Giroud-Godquin, A. M.; Marchon, J. C.; Guillon, D.; Skoulios, A. *Chem. Phys. Lett.* **1989**, *157*, 552. (e) Barberá, J.; Esteruelas, M. A.; Levelut, A. M.; Oro, L. A.; Serrano, J. L.; Sola, E. *Inorg. Chem.* **1992**, *31*, 732.

(7) (a) Zimmermann, H.; Poupko, R.; Luz, Z.; Billard, J. Z. *Naturforsch.* **1985**, *40a*, 149. (b) Zimmermann, H.; Poupko, R.; Luz, Z.; Billard, J. *Liq. Cryst.* **1988**, *3*, 759. (c) Budig, H.; Lunckwitz, R.; Paschke, R.; Tschierske, C.; Nütz, U.; Diele, S.; Pelzl, G. *J. Mater. Chem.* **1996**, *6*, 1283. (d) Lunckwitz, R.; Tschierske, C.; Diele, S. *J. Mater. Chem.* **1997**, *7*, 2001. (e) Jakli, A.; Saupe, A.; Scherowsky, G.; Chen, X. H. *Liquid Crystals* **1997**, *22*, 309.

(8) (a) Malthête, J.; Collet, A. *Nouv. J. Chim.* **1985**, *9*, 151. (b) Levelut, A. M.; Malthête, J.; Collet, A. *J. Physique* **1986**, *47*, 351. (c) Malthête, J.; Collet, A. *J. Am. Chem. Soc.* **1987**, *109*, 7544.

(9) (a) Lei, L. *Mol. Cryst. Liq. Cryst.* **1987**, *146*, 41. (b) Leung, K. M.; Lei, L. *Mol. Cryst. Liq. Cryst.* **1987**, *146*, 71. (c) Cometti, G.; Dalcanale, E.; Duvoisel, A.; Levelut, A. M. *J. Chem. Soc. Chem. Commun.* **1990**, 163. (d) Xu, B.; Swager, T. M. *J. Am. Chem. Soc.* **1993**, *115*, 1159. (e) Xu, B.; Swager, T. M. *J. Am. Chem. Soc.* **1995**, *117*, 5011.

(10) Zheng, H.; Swager, T. M. *J. Am. Chem. Soc.* **1994**, *116*, 761.

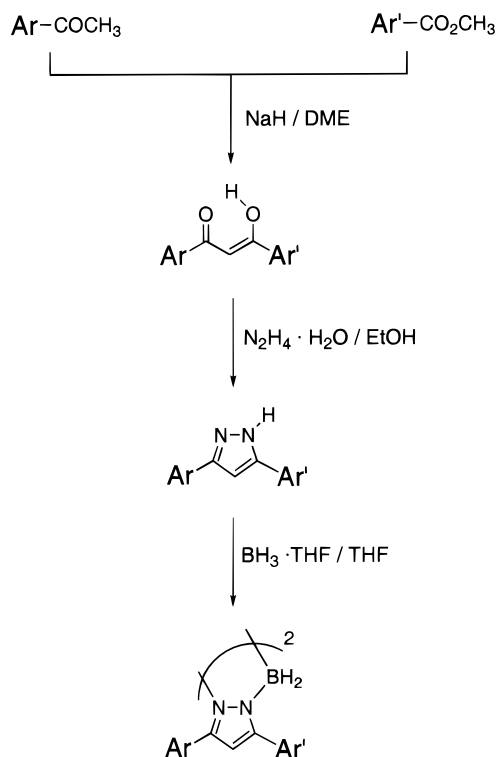


**Figure 2.** Synthetic route to the alkoxyphenyl-substituted pyrazaboles.

## Results

**Synthesis and Characterization.** The synthetic route followed to obtain the pyrazabole derivatives is shown in Figure 2. The precursory  $\beta$ -diketones were obtained by the acylation reaction of methyl ketones using the appropriate acetophenone and the appropriate methyl ester. The reaction takes place in the presence of sodium hydride as a base and DME as a solvent (DME = 1,2-dimethoxyethane). Neither the acetophenones nor the methyl esters were commercially available, so each precursor was prepared from commercially available compounds using the most adequate procedure in each case.  $\beta$ -diketones were made to react with hydrazine hydrate to obtain the derived pyrazoles. Finally, the pyrazabole ring is prepared from the precursory pyrazole using borane–THF complex in THF as the solvent under reflux (THF = tetrahydrofuran), using a modification of the procedure described by Trofimenko.<sup>11</sup>

From the  $^1\text{H}$  NMR spectra we conclude that all the  $\beta$ -diketones studied are in the enol form in  $\text{CDCl}_3$  solution. A singlet is found in the region 6.6–7.1 ppm which corresponds to the proton of the  $-\text{CH}=\text{}$  group of the 1,3-propanedione system. Another singlet is observed at 17.0–17.2 ppm assigned to the proton of the enol OH group. Each of these signals integrate one proton. Moreover, no peak is found in the region between 4.5 and 5.5 ppm, so the presence of  $\text{CH}_2$  of the keto form can be discarded.

In the pyrazoles, the signal of the NH proton does not appear except for the compound with four hexyloxy

chains where it can be seen as a very broad peak between 10.0 and 10.7 ppm.

The infrared spectra of the pyrazaboles show the stretching bands characteristic of the B–H bonds at  $2500\text{--}2400\text{ cm}^{-1}$ . However, these protons are not detected in NMR, as they should give an extremely broad band masked by the other peaks of the spectrum.<sup>11b</sup> The  $^1\text{H}$  NMR of the symmetrically substituted pyrazaboles (same substitution on all phenyl rings) reveal the equivalence of the 2 and 6 positions of the pyrazabole cycle (C–H proton of each pyrazole ring), in such a way that the protons placed in these positions originate only a singlet at about 6.3–6.4 ppm. When the pyrazaboles are unsymmetrically substituted, the protons of the pyrazabole cycle (protons j, j' in Figures 3 and 4) give rise to two singlets in the region of 6.3–6.4 ppm, which correspond to each of two different regioisomers designed as cis and trans in proportion 1/1 for **10C<sub>10</sub>** and 2/1 or 1/2 for **12C<sub>10</sub>unsym**. Moreover, the benzene protons placed in *ortho* position to the pyrazabole ring are splitted in the same ratio (protons f, f', m, m', n, n' in Figure 3 and protons g, g', m, m' in Figure 4).

**Optical Microscopy and DSC Study.** All the pyrazaboles prepared as well as the precursory  $\beta$ -diketones and pyrazoles have been studied by optical microscopy with polarized light and a heating–cooling stage, and by DSC. None of the precursory  $\beta$ -diketones display liquid crystal behavior, which is in accordance with previous studies of alkoxy-substituted  $\beta$ -diketones derived from 1,3-diphenyl-1,3-propanedione.<sup>4,12</sup> The only precursory pyrazole to exhibit liquid crystal behavior is 3,5-bis(4'-decyloxyphenyl)pyrazole which shows classical calamitic smectic A and C mesophases, as reported previously.<sup>4</sup> The molecules of this compound have an elongated shape, called *banana*-like. The pyrazoles with more than two aliphatic chains are not mesomorphic. In this case, the presence of four, five, or six hydrocarbon chains precludes calamitic mesomorphism, and hydrogen bonding does not generate disk-shaped dimeric entities capable of yielding columnar mesomorphism. Despite their low tendency to mesomorphism, several pyrazoles show polymorphism in the solid state, thus giving a number of crystal–crystal transitions before melting.

Three of the pyrazaboles prepared display columnar mesomorphism (see Table 2). The rest of them only display crystal–crystal and/or crystal–isotropic liquid transitions, that are in most cases lower than  $100\text{ }^\circ\text{C}$ .

Compound **8C<sub>10</sub>** shows a monotropic mesophase. In the polarizing optical microscope, a birefringent fluid phase is observed with a pseudo-focal-conic texture. Its fluidity and its texture is characteristic of a disordered hexagonal columnar mesophase ( $\text{Col}_{\text{hd}}$ ). In the DSC thermogram, the isotropic liquid-to-mesophase transition appears as an exothermic peak at  $46.3\text{ }^\circ\text{C}$  with a small transition enthalpy ( $0.5\text{ kJ mol}^{-1}$ , see Table 2). This supports the identification of the discotic mesophase as disordered (without a constant stacking distance). Unfortunately, the mesophase can only be observed by supercooling the isotropic liquid and crystallizes very

(11) (a) Trofimenko, S. *J. Am. Chem. Soc.* **1966**, *88*, 1842. (b) Trofimenko, S. *J. Am. Chem. Soc.* **1967**, *89*, 3165. (c) Trofimenko, S. *J. Am. Chem. Soc.* **1967**, *89*, 4948. (d) Trofimenko, S. *Inorg. Synth.* **1970**, *12*, 99.

(12) (a) Tantrawong, S.; Styring, P.; Goodby, J. W. *J. Mater. Chem.* **1993**, *3*, 1209. (b) Zheng, H.; Lai, C. K.; Swager, T. M. *Chem. Mater.* **1995**, *7*, 2067.

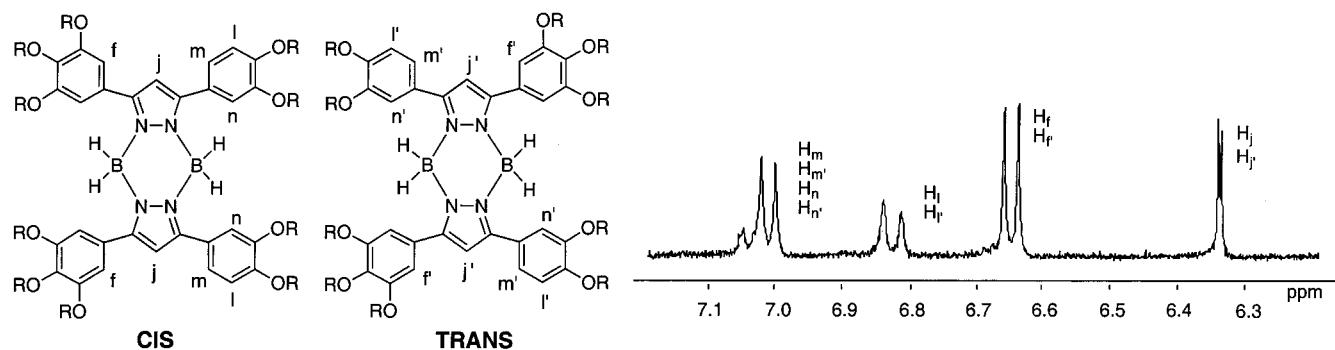


Figure 3. Cis and trans regioisomers and aromatic region of the  $^1\text{H}$  NMR spectrum of compound  $10\text{C}_{10}$ .

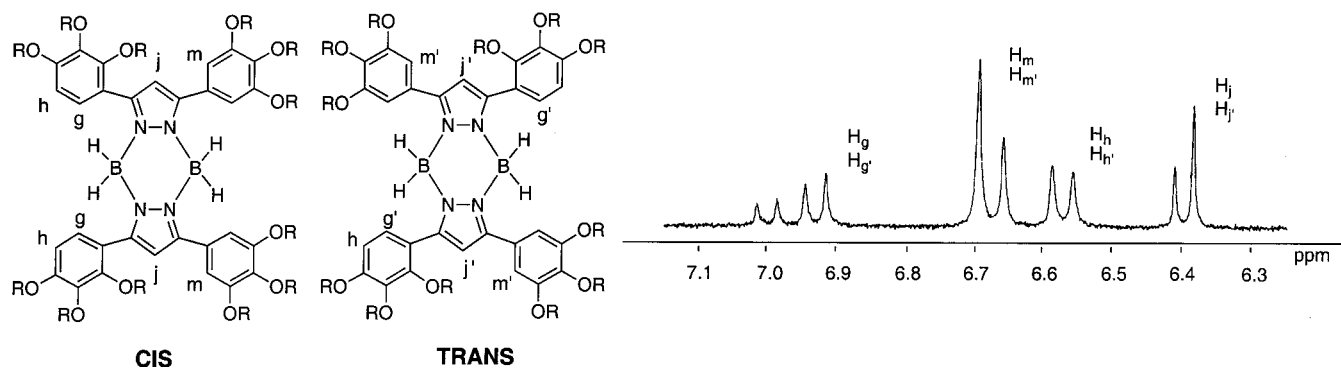


Figure 4. Cis and trans regioisomers and aromatic region of the  $^1\text{H}$  NMR spectrum of compound  $12\text{C}_{10}\text{unsym}$ .

Table 2. Optical, Thermal, and Thermodynamical Properties of the Alkoxy-substituted Pyrazoboles.

compound	transition	$T$ ( $^{\circ}\text{C}$ )	$\Delta H$ ( $\text{kJ mol}^{-1}$ )
$4\text{C}_{10}$	$\text{C}_1\text{-C}_2^a$	106.3	22.6
	$\text{C}_2\text{-I}$	166.6	42.5
$8\text{C}_6\text{-3,4}$	$\text{C}_1\text{-C}_2^a$	84.2	22.7
	$\text{C}_2\text{-I}$	111.3	17.6
$8\text{C}_{10}\text{-3,4}$	$\text{C}_1\text{-C}_2^a$	66.5	20.0
	$\text{C}_2\text{-I}$	82.8	40.8
	$\text{I-Col}_{\text{hd}}^b$	46.3	0.5
$8\text{C}_{14}\text{-3,4}$	$\text{C-I}$	82.9	84.2
$8\text{C}_{10}\text{-3,5}$	$\text{C-I}$	55.9	40.5
$10\text{C}_6$	$\text{C-I}$	60.1	32.4
$10\text{C}_{10}$	$\text{C}_1\text{-C}_2$	36.4	96.1
	$\text{C}_2\text{-I}^c$	47.1	
	$\text{Col}_{\text{hd}}\text{-I}^d$	30.8	1.5
$10\text{C}_{14}$	$\text{C-I}$	43.4	124.6
$12\text{C}_{10}\text{unsym}$	$\text{Col}_{\text{hd}}\text{-I}$	51.0	2.9
$12\text{C}_{10}\text{sym}$	$\text{C}_1\text{-C}_2$	34.9	67.8
	$\text{C}_2\text{-I}$	45.9	33.5

<sup>a</sup> Transition only observed on the first heating. <sup>b</sup> Monotropic transition. <sup>c</sup> Transitions shown by the sample crystallized after several days at room temperature. <sup>d</sup> Transition also observed upon heating a freshly prepared sample.

quickly. This fact precluded the study of the mesophase by X-ray diffraction.

Pyrazobole  $10\text{C}_{10}$  exhibits a liquid crystal phase at room temperature. Although this phase is metastable, it can be maintained at room-temperature several days before slow crystallization takes place. Columnar mesophases at low temperatures are not very common, and only a few cases have been described in the literature.<sup>2b,3,6e,9a,12b,13</sup> A freshly prepared sample of  $10\text{C}_{10}$  exhibits a single peak at  $30.8\text{ }^{\circ}\text{C}$ , with a transition enthalpy of  $1.5\text{ kJ mol}^{-1}$  (see Table 2), which corresponds to the mesophase-to-isotropic liquid transition. In the cooling scan (at  $10\text{ }^{\circ}\text{C min}^{-1}$ ) no transition is observed. In the microscope, it is observed that the freshly prepared compound is in a birefringent fluid

phase. After heating into the isotropic liquid, reappearance of the mesophase in the cooling process is very slow. A pseudo-focal-conic texture grows slowly at an optimal temperature of about  $22\text{ }^{\circ}\text{C}$ . After several hours at this temperature, the texture looks as presented in Figure 5. The observed texture and the transition enthalpy value suggests that the mesophase is disordered hexagonal columnar. Being kinetically stable for several days, an X-ray diffraction study of this mesophase was possible (see next section).

Compound  $12\text{C}_{10}\text{unsym}$  displays a thermodynamically stable mesophase at room temperature. The compound shows a single DSC peak at  $51.0\text{ }^{\circ}\text{C}$  with a transition enthalpy of  $2.9\text{ kJ mol}^{-1}$  (see Table 2). In the cooling cycle only the isotropic liquid-to-mesophase transition is observed, and crystallization does not take place even at very low temperatures (cooling to  $-70\text{ }^{\circ}\text{C}$ ). In contrast to  $10\text{C}_{10}$ , this compound does not crystallize in the course of time. Under the microscope a pristine sample of  $12\text{C}_{10}\text{unsym}$  is fluid and does not exhibit a characteristic texture. After the fluid is heated into the isotropic liquid, during the cooling process, a texture is developed with homeotropic and pseudo-focal-conic regions. From this texture and from the transition enthalpy, it is concluded that the liquid crystal phase is disordered hexagonal columnar. This assignment was confirmed by the X-ray diffraction study performed on the mesophase (see next section).

**X-ray Diffraction Study on the Mesophase.** The mesophases of  $10\text{C}_{10}$  and  $12\text{C}_{10}\text{unsym}$  were studied by powder X-ray diffraction at room temperature in a Guinier diffractometer and in a pinhole camera. The X-ray patterns obtained for the two compounds contain a sharp and strong peak in the small-angle region. By using Bragg's law, this maximum gives a spacing of  $26.0\text{ \AA}$  for  $10\text{C}_{10}$  and  $24.7\text{ \AA}$  for  $12\text{C}_{10}\text{unsym}$ . In addition,

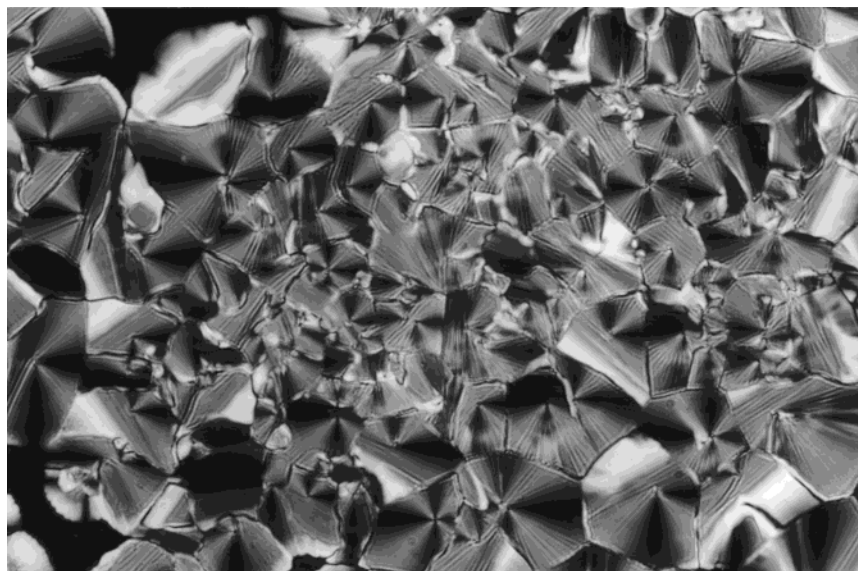


**Figure 5.** Microphotograph showing the texture of the Col<sub>hd</sub> mesophase of **10C<sub>10</sub>** under polarized light.

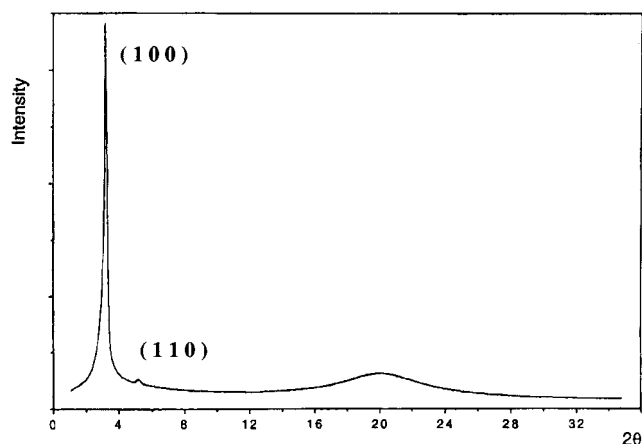


**Figure 6.** Diffraction pattern of the Col<sub>hd</sub> mesophase of compound **12C<sub>10</sub>unsym** at room temperature.

in the latter compound, a weak peak is observed at a slightly larger angle, which corresponds to a spacing of 14.3 Å (Figure 6). This distance and the first spacing (24.7 Å) are in the ratio 1:√3, typical of a hexagonal lattice in which the two maxima correspond to the (1 0 0) and (1 1 0) reflections. The pattern is characteristic of a hexagonal columnar mesophase and this confirms the microscope and DSC observations. The hexagonal lattice constant (intercolumnar distance) deduced from the pattern is  $a = 28.5$  Å for **12C<sub>10</sub>unsym**. Although for **10C<sub>10</sub>**, the presence of only a maximum at small angles does not allow the unambiguous determination of the mesophase structure; from the similarity of the chemical structures and microscope textures, as well as from the transition enthalpy value, it can be concluded that the mesophase is of the same type as that of **12C<sub>10</sub>unsym**. With the assignment of the 26.0 Å maximum to the (1 0 0) reflection from the hexagonal lattice, the intercolumnar distance is in this case  $a = 30.0$  Å (calculated as  $a = 26.0 \times 2/\sqrt{3}$ ). The absence of other reflections at low diffraction angles apart from the (1 0 0) reflection is frequent in diffraction patterns of hexagonal columnar mesophases,<sup>14</sup> and it is due to a minimum in the form factor, which precludes the observation of peaks in this angle region.

At high angles, a broad and diffuse halo centered at 4.5 Å is observed (see Figure 6), characteristic of the interferences between the conformationally disordered hydrocarbon chains. The absence of Bragg peaks in this region confirms the description of the columnar mesophase of these compounds as *disordered*: i.e., there is no X-ray reflection corresponding to intracolumnar order. Although the intermolecular distance inside the columns cannot be measured because of the absence of regular stacking, it can be predicted that the mean intermolecular distance will be shorter for **10C<sub>10</sub>** than for **12C<sub>10</sub>unsym** as in the latter a smaller intercolumnar distance has been obtained despite the greater molecule size. Assuming that the density of the compounds in the mesophase is near  $1 \text{ g cm}^{-3}$ , an estimation of the mean stacking distance  $c$  can be made on the basis of the following equation:

$$\rho = (MN)/V$$

where  $M$  is the molar mass in g (2025 for **10C<sub>10</sub>** and 2339 for **12C<sub>10</sub>unsym**);  $N$ , the Avogadro number; and  $V$ , the unit cell volume (in cm<sup>3</sup>). From the calculated  $V$  values ( $3362 \times 10^{-24}$  cm<sup>3</sup> for **10C<sub>10</sub>** and  $3717 \times 10^{-24}$  cm<sup>3</sup> for **12C<sub>10</sub>unsym**),  $c$  can be estimated on the basis of the following equation:

$$V = (\sqrt{3}/2) a^2 (c \times 10^{-24})$$

where  $a$  is the hexagonal lattice constant (in Å) measured by X-ray diffraction. The deduced mean stacking distance is about 4.3 Å for **10C<sub>10</sub>** and about 5.3 Å for **12C<sub>10</sub>unsym**. The greater estimated distance for the

(13) (a) Kohne, B.; Praefcke, K.; Stephan, W. *Chimia* **1986**, *40*, 14. (b) Strzelecka, H.; Jallabert, C.; Veber, M.; Davidson, P.; Levelut, A. M. *Mol. Cryst. Liq. Cryst.* **1988**, *161*, 395. (c) Malthête, J.; Levelut, A. M. *Adv. Mater.* **1991**, *3*, 94. (d) Barberá, J.; Cativiela, C.; Serrano, J. L.; Zurbano, M. M. *Adv. Mater.* **1991**, *3*, 602. (e) Zheng, H.; Xu, B.; Swager, T. M. *Chem. Mater.* **1996**, *8*, 907.

(14) (a) Cafagna, C.; Roviello, A.; Sirigu, A. *Mol. Cryst. Liq. Cryst.* **1985**, *122*, 151. (b) Gramsbergen, E. F.; Hoving, H. J.; de Jeu, W. H.; Praefcke, K.; Kohne, B. *Liq. Cryst.* **1986**, *1*, 397. (c) Metersdorf, H.; Ringsdorf, H. *Liq. Cryst.* **1989**, *5*, 1757. (d) Zheng, H.; Carroll, P. J.; Swager, T. M. *Liq. Cryst.* **1993**, *14*, 1421.

latter compound can be explained by the greater spatial requirements of its 12 paraffinic chains.

### Discussion

Only pyrazaboles possessing 8, 10, and 12 decyloxy groups display mesomorphism (compounds **8C<sub>10</sub>-3,4**, **10C<sub>10</sub>**, and **12C<sub>10</sub>unsym**). From the data in Table 2, it can be deduced that an increase in the number of aliphatic chains diminishes the transition temperatures. Thus, among the pyrazaboles containing decyloxy chains, the one with four chains (**4C<sub>10</sub>**) has the highest melting point, and this magnitude gradually decreases on passing to 8 (**8C<sub>10</sub>-3,4**, and **8C<sub>10</sub>-3,5**), 10 (**10C<sub>10</sub>**), and 12 chains (**12C<sub>10</sub>sym**).

Another important point in the occurrence of mesomorphism is the position of the alkoxy substituents. If we compare again the derivatives with decyloxy groups, it can be observed that symmetrical substitution in the phenyl rings does not lead to mesomorphism: substitution in 4 and 4' (**4C<sub>10</sub>**), 3,5 and 3',5' (**8C<sub>10</sub>-3,5**), and 3,4,5 and 3',4',5' (**12C<sub>10</sub>sym**). On the other hand, unsymmetrical substitution in each phenyl ring promotes mesomorphism: substitution in 3,4 and 3',4' (**8C<sub>10</sub>-3,4**), 3',4' and 3,4,5 (**10C<sub>10</sub>**), and 2,3,4 and 3',4',5' (**12C<sub>10</sub>unsym**). Thus, the decrease in the molecule symmetry is a favorable element for the appearance of columnar mesophases in these kind of compounds. Indeed, a higher symmetry produces a better packing in the solid state and stabilizes the crystalline phases to the detriment of the mesomorphic phases. We observe this effect when we compare the absence of mesomorphism in **8C<sub>10</sub>-3,5** (substitution in 3,5 and 3',5') with the monotropic Col<sub>hd</sub> mesomorphism in **8C<sub>10</sub>-3,4** (substitution in 3,4 and 3',4'), and even more clearly by comparing the absence of mesomorphism in **12C<sub>10</sub>sym** (substitution in 3,4,5 and 3',4',5') with the enantiotropic Col<sub>hd</sub> mesomorphism in **12C<sub>10</sub>unsym** (substitution in 2,3,4 and 3',4',5').

By comparing the phase behavior of the mesogenic derivatives, we can notice that passing from 8 (**8C<sub>10</sub>-3,4**) to 10 chains (**10C<sub>10</sub>**) is very efficient in stabilizing the discotic mesophase and enhances its temperature range. Upon increasing the number of chains, the flexible region of the molecule increases. Thus, the hydrocarbon groups arrange themselves better around the rigid core, which favors columnar mesomorphism. Probably, for this reason neither the compound with four chains **4C<sub>10</sub>** nor the compound with eight chains **8C<sub>10</sub>-3,5** is mesogenic, as this number is insufficient to fill the space around the central core. An increase of the number of hydrocarbon chains from 8 to 10 (**10C<sub>10</sub>**) not only expands the flexible region of the molecule but also reduces the molecular symmetry and consequently the melting point, all of which enhances the mesophase range. It must also be remembered that the latter compound consists of a mixture of two regioisomers, as has been described above. The same trend is observed on increasing the number of side groups from 10 (**10C<sub>10</sub>**) to 12 with substitution in 2,3,4 and 3',4',5' (**12C<sub>10</sub>unsym**).

As far as the chain length is concerned, mesomorphic properties are only observed when the compounds contain decyloxy chains. This can be explained in terms of the requirement of an equilibrated balance between the size of the central rigid core and the size of the

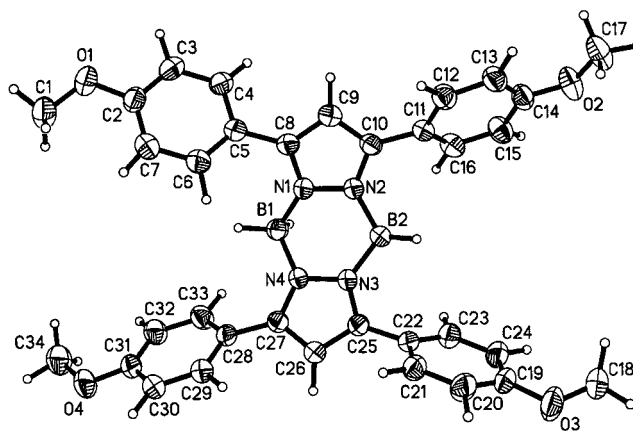


**Figure 7.** View of the molecular structure of one independent molecule of **4C<sub>1</sub>** together with the atomic numbering scheme used.

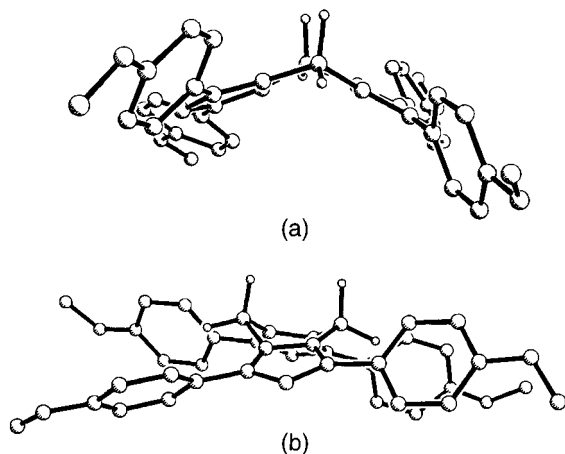
paraffinic crown. When the side chains are too short or too long they are not able to appropriately fill the space around the core and this hinders columnar mesomorphism. In the case of the hexyloxy-substituted pyrazaboles, the absence of mesomorphism is related with the increase of the melting points compared to the decyloxy-substituted homologues (see Table 2). When the side chains are tetradecyloxy groups, the melting points are similar to those of the decyloxy homologues, but the former crystallizes at higher temperatures on cooling, which precludes the occurrence of monotropic mesomorphism.

**Crystal Structure of 4C<sub>1</sub>.** With the aim of gaining insight into the molecular structure of these compounds, we tried to obtain single crystals of some members of this series. Let us recall that no single-crystal X-ray analysis of a pyrazabole with BH<sub>2</sub> as bridging group has been described in the literature. The knowledge of the molecule organization in the solid state should help in the understanding of the molecule packing in the mesophase. Unfortunately all attempts to obtain single crystals were unsuccessful, probably due to the presence in these molecules of long hydrocarbon chains, that make the obtention of X-ray-quality crystals difficult. Therefore, we decided to obtain single crystals of a model compound that possesses the same central core and methoxy groups as substituents: 1,3,5,7-tetrakis-(4'-methoxyphenyl)pyrazabole (**4C<sub>1</sub>**). This compound was prepared by the same reaction sequence described above for the long-chain homologues using methyl 4-methoxybenzoate and 4-methoxyacetophenone as starting materials. As expected, the absence of long hydrocarbon chains made the obtention of a single-crystal possible, one of which was selected for the X-ray analysis.

The crystal structure was solved by direct methods using the SHELXS-86 program and refined using the SHELX-93 program to  $R_1 = 0.0438$ . 4694 reflections were measured (3890 independent) in the range  $3^\circ \leq \theta \leq 45^\circ$  in a Siemens P4 diffractometer operating with a Mo K $\alpha$  beam ( $\lambda = 0.71073$  Å). **4C<sub>1</sub>** crystallizes in a triclinic cell, space group  $P\bar{1}$ , with lattice constants  $a = 10.093(2)$  Å,  $b = 11.634(2)$  Å,  $c = 13.574(3)$  Å,  $\alpha = 81.71(3)^\circ$ ,  $\beta = 74.63(3)^\circ$ ,  $\gamma = 78.85(3)^\circ$ ,  $V = 1500.5(5)$  cm<sup>3</sup>,  $Z = 2$ . The molecular structure is depicted in Figure 7, and the significant bond distances, bond

**Table 3.** Selected Bond Distances (Å), Bond Angles (deg) and Dihedral Angles (deg) for Compound **4C<sub>1</sub>**

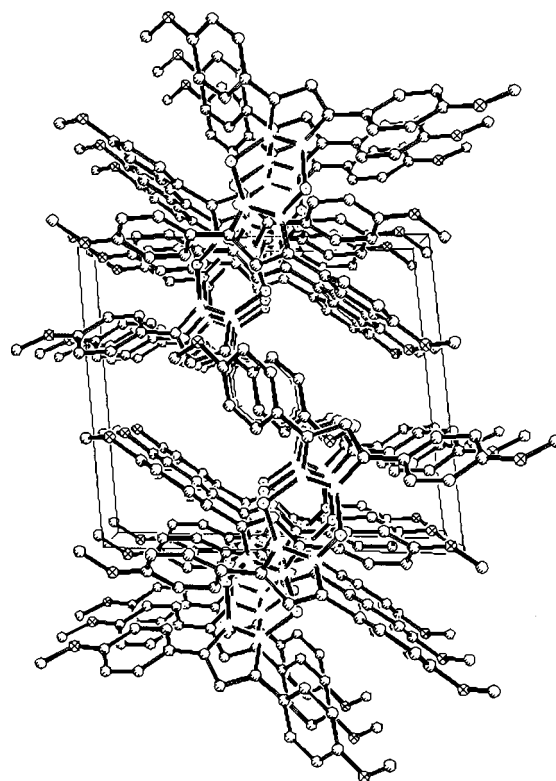
B(1)–N(1)	1.573(3)	B(2)–N(2)	1.571(3)
B(1)–N(4)	1.557(3)	B(2)–N(3)	1.560(3)
B(1)–H(1)	1.098(5)	B(2)–H(2)	1.183(4)
B(1)–H(1')	1.179(5)	B(2)–H(2')	1.126(4)
N(1)–N(2)	1.368(2)	N(3)–N(4)	1.370(2)
N(1)–B(1)–N(4)	105.2(2)	N(2)–B(2)–N(3)	105.9(2)
H(1)–B(1)–H(1')	114.6(4)	H(2)–B(2)–H(2')	114.6(3)
B(1)–N(1)–N(2)	117.0(2)	B(2)–N(2)–N(1)	119.7(2)
B(1)–N(4)–N(3)	117.6(2)	B(2)–N(3)–N(4)	120.0(2)
B(1)–N(1)–N(2)–B(2)	–18.0(3)		
B(2)–N(3)–N(4)–B(1)	–9.9(3)		

**Figure 8.** View of the molecular structure of **4C<sub>1</sub>**: (a) along the *b* axis and (b) along the *c* axis.

angles, and dihedral angles are listed in Table 3.

From the bond angles in Table 3 it is deduced that the boron atoms have tetrahedral coordination, with some distortion in the sense that the hydrogen–boron–hydrogen angles ( $114.6(4)^\circ$  and  $114.6(3)^\circ$ ) are larger than the nitrogen–boron–nitrogen angles ( $105.0(2)^\circ$  and  $105.7(2)^\circ$ ). One of the most significant characteristics of the molecular geometry is that the central ring formed by the two boron atoms and the four nitrogen atoms adopts a folded conformation close to a slightly twisted boat structure. This can be easily observed when the molecule is viewed from other perspectives, such those represented in Figure 8. The dihedral angle between the mean plane passing through B(1), N(1), N(2), and B(2) and the one passing through B(1), N(4), N(3), and B(2) is  $130.7(1)^\circ$ . This means that the central part of the molecule has approximately a *roof* shape, each of whose slopes contains a pyrazole ring, with the boron atoms placed on the top. The benzene rings and the pyrazole ring to which they are bonded are not coplanar but are rotated by an angle comprised between  $32.81(8)^\circ$  and  $48.33(9)^\circ$ . The deformation from the ideal boat structure is put in evidence by the dihedral angles B(1),N(1),N(2),B(2), with a value of  $-18.0(3)^\circ$ , and B(1),N(4),N(3),B(2), with a value of  $-9.9^\circ$ . It is also noticeable that that two of the boron–nitrogen bond distances are significantly longer than the other two (Table 3).

The presence in the unit cell of two molecules related by a symmetry center implies an antiparallel arrangement, promoted by the peculiar molecule geometry. A stacking effect takes place that gives rise to a columnar structure (Figure 9) in which the molecular centroids are not exactly put in line, but shifted to both sides of

**Figure 9.** Representation of the columnar packing observed in the crystal structure of compound **4C<sub>1</sub>** along the *a* axis.

the columnar axis (*a* axis of the unit cell) in an alternating way. Although the results of this study must be cautiously extrapolated to the mesophase, they make evident that these molecules have tendency to generate columnar structures in the solid state. In **4C<sub>1</sub>** the absence of long hydrocarbon chains precludes the occurrence of mesophase after melting. However, in the analogous compounds with long chains liquid crystal behavior is possible because the presence of the paraffinic crown provides the molecule with the necessary requirements to generate discotic mesomorphism, which is not incompatible with the folded shape of the pyrazabole ring. Nevertheless, it is possible that in the mesomorphic state the enhanced conformational freedom allows the inversion of the boat structure, or even the adoption of other conformations such as flat or chair. These structures have been found in the crystal structures of other pyrazaboles with non-hydrogen substituents bonded to the boron atoms.<sup>5</sup>

## Conclusions

This work has shown that the dimerization of half-disk-shaped nonmesogenic pyrazaboles through  $\text{BH}_2$  bridges leads to pyrazaboles with liquid crystal properties. Three compounds in the series show hexagonal columnar mesomorphism at temperatures below  $51^\circ\text{C}$ . **8C<sub>10</sub>-3,4** displays a monotropic hexagonal columnar mesophase that crystallizes very quickly, **10C<sub>10</sub>** exhibits a kinetically stable mesophase that can be kept at room temperature for several days, and **12C<sub>10</sub>unsym** shows a thermodynamically stable mesophase at room temperature. In the two last cases, the kind of mesophase has been confirmed by X-ray diffraction.

From the study of several pyrazaboles with different position, length, and number of alkyl chains, we con-

clude that an increase in the number of the side chains decreases the melting points, and in the case of mesogenic compounds enhances the thermal range of the mesophase as the larger number of hydrocarbon chains produces a more cylindrical symmetry in the molecule. The positions of the decyloxy groups in the aromatic rings of the pyrazabole have also a crucial influence on the appearance of columnar mesophases in these derivatives, and substitutions that reduce the molecular symmetry favor mesomorphism. This is probably the reason **12C<sub>10</sub>sym** does not show liquid crystal properties, whereas its isomer with nonsymmetrical substitution, **12C<sub>10</sub>unsym**, does.

Finally, the first crystal structure of a pyrazabole nonsubstituted at the boron atoms is presented (**4C<sub>1</sub>**). Although this compound is not liquid crystalline, it shows a columnar packing in the solid state that supports the ability of the long-chain homologues to self-arrange in columnar mesophases.

## Experimental Section

**General Methods.** Microanalyses were performed with a Perkin-Elmer 240C microanalyzer. <sup>1</sup>H NMR spectra were recorded on a Varian Unity 300 spectrometer. IR spectra were obtained on a Perkin-Elmer 1600 (FTIR series) spectrometer. Mass spectra were obtained on a VG Autospec EBE (FAB<sup>+</sup>, 3-NBA matrix). The optical textures of the mesophases were studied with an Olympus polarizing microscope equipped with a Linkam THMS 600 hot stage, a TMS 91 central processor, and a CS196 cooling stage. The transition temperatures were measured by differential scanning calorimetry with a Perkin-Elmer DSC-7 operated at a scanning rate of 10° min<sup>-1</sup> on heating. The apparatus was calibrated with indium (156.6 °C, 28.4 J g<sup>-1</sup>) and *n*-octane (-56.7 °C, 176.39 J g<sup>-1</sup>) as standards. X-ray diffraction patterns were obtained using a pinhole camera (Anton-Paar) and a Guinier diffractometer (Huber 644). The former operates with a point-focused Ni-filtered Cu K $\alpha$  beam. The sample was held in Lindemann glass capillaries (1 mm diameter) and heated with a variable-temperature attachment. The diffraction pattern was collected on flat photographic film. The Guinier diffractometer uses Cu K $\alpha$  radiation monochromatized by a germanium crystal.

**Synthesis of the Precursors.** All the **methyl benzoate ester derivatives**, the **4-*n*-decyloxyacetophenone**, and **3,5-di-*n*-decyloxyacetophenone** were prepared by Williamson alkylation of the commercially available hydroxybenzoate or hydroxyacetophenone derivatives following literature methods.<sup>15</sup> **3,4-Di-*n*-alkoxyacetophenones** and **2,3,4-tri-*n*-decyloxyacetophenone** were prepared in two steps adapting literature methods: alkylation of the pyrocatechol or the pyrogallol in a similar way as described above, and Friedel-Crafts acylation. A typical procedure for the last step is as follows:

**2,3,4-Tri-*n*-decyloxyacetophenone.** A total of 19 mmol (2.53 g) of aluminum trichloride, 18 mmol (10.58 g) of 1,2,3-tri-*n*-decyloxybenzene, and 110 mL of dry dichloromethane were cooled at -5 °C using a NaCl-ice bath. A total of 20 mmol (1.57 g) of acetyl chloride was added dropwise. The mixture was allowed to reach room temperature and was stirred a maximum of 3 h. Then, the reaction was worked up by pouring it into cold diluted HCl (100 mL of concentrated HCl and 200 g of ice). The organic layer was separated and washed successively with diluted HCl 2 N (1  $\times$  100 mL), saturated NaHCO<sub>3</sub> (3  $\times$  100 mL), and H<sub>2</sub>O (3  $\times$  100 mL). After the organic layer was dried (MgSO<sub>4</sub>), the solvent was evaporated and the residue purified by silica column chromatography using hexane/EtOAc (3/2) as the eluent. Yield: 47%. The

product is a light yellow oil. IR (Nujol, NaCl):  $\nu$ (C=O) 1674,  $\nu$ (arC-C) 1587,  $\nu$ (C-O) 1285. <sup>1</sup>H NMR (CDCl<sub>3</sub>, 293 K):  $\delta$  0.84-0.88 (m, 9H), 1.25-1.46 (m, 42H), 1.75-1.79 (m, 6H), 2.59 (s, 3H), 3.88-3.97 (m, 4H), 4.07 (t,  $J$  = 6.8 Hz, 2H), 6.66 (d,  $J$  = 8.8 Hz, 1H), 7.46 (d,  $J$  = 8.8 Hz, 1H).

**3,4,5-Tri-*n*-decyloxyacetophenone** was synthesized using 3,4,5-*tri-n*-decyloxybenzoic acid and adapting literature methods.<sup>16</sup> A total of 5.08 mmol (3.0 g) of 3,4,5-*tri-n*-decyloxybenzoic acid was dissolved in 40 mL of dry THF and cooled at 0 °C. A total of 20.3 mmol (12.7 mL, 1.6 M in Et<sub>2</sub>O) of methyllithium was added quickly. The mixture was stirred 2 h at 0 °C. Then, 0.1 mol (12.7 mL) of freshly distilled chlorotrimethylsilane was added. The reaction was allowed to reach room temperature and 40 mL of HCl 1 N was added. The resulting mixture was poured into Et<sub>2</sub>O (30 mL), and the organic layer was separated and washed with 20 mL of H<sub>2</sub>O. After the organic layer was dried over MgSO<sub>4</sub>, the solvent was removed and the residue was purified by silica column chromatography using hexane/EtOAc (40/1) as the eluent. Yield: 85%. White solid. Mp: 43 °C. IR (Nujol, NaCl):  $\nu$ (C=O) 1668,  $\nu$ (arC-C) 1584,  $\nu$ (C-O) 1234, 1211. <sup>1</sup>H NMR (CDCl<sub>3</sub>, 293 K):  $\delta$  0.86 (t,  $J$  = 6.5 Hz, 9H), 1.25-1.45 (m, 42H), 1.65-1.80 (m, 6H), 2.54 (s, 3H), 4.00 (t,  $J$  = 6.3 Hz, 6H), 7.15 (s, 2H).

All the  **$\beta$ -diketones**<sup>4,12b,17</sup> and **pyrazoles**<sup>4</sup> were synthesized by using literature procedures. Spectroscopic data for some new selected compounds follows.

**1-(2',3',4'-Tri-*n*-decyloxyphenyl)-3-(3'',4'',5''-Tri-*n*-decyloxyphenyl)-1,3-propanodione.** Anal. Calcd for C<sub>75</sub>H<sub>132</sub>O<sub>8</sub>: C, 77.53; H, 11.45. Experimental: C, 77.93; H, 11.16. IR (Nujol, NaCl):  $\nu$ (O-H) 3357,  $\nu$ (C=O) 1594,  $\nu$ (C=C) 1594,  $\nu$ (C-O) 1297. <sup>1</sup>H NMR (CDCl<sub>3</sub>, 293 K):  $\delta$  0.82-0.90 (m, 18H), 1.19-1.50 (m, 84H), 1.68-1.86 (m, 12H), 3.96-4.05 (m, 12H), 6.72 (d,  $J$  = 9.0 Hz, 1H), 7.15 (s, 1H), 7.17 (s, 2H), 7.65 (d,  $J$  = 9.0 Hz, 1H), 17.10 (s, 1H). MS  $m/z$  (%): 1162 (23, [M<sup>+</sup>]), 574 (100), 433 (80).

**3(5)-(2',3',4'-Tri-*n*-decyloxyphenyl)-5(3)-(3'',4'',5''-tri-*n*-decyloxyphenyl)pyrazole.** IR (Nujol, NaCl):  $\nu$ (N-H) 3112,  $\nu$ (C=N, arC-C) 1607, 1588, 1492,  $\nu$ (C-O) 1241. <sup>1</sup>H NMR (CDCl<sub>3</sub>, 293 K):  $\delta$  0.84-0.88 (m, 18H), 1.25-1.47 (m, 84H), 1.71-1.80 (m, 12H), 3.94-4.11 (m, 12H), 6.70 (d,  $J$  = 8.8 Hz, 1H), 6.71 (s, 1H), 7.04 (s, 2H), 7.31 (d,  $J$  = 8.8 Hz, 1H). MS  $m/z$  (%): 1158 (100, [M<sup>+</sup>]), 1018 (28).

**General Procedure for the Synthesis of the Pyrazaboles.** A total of 1 mmol of the appropriate pyrazole and 5 mL of dry THF were refluxed 30 min under an argon atmosphere. Afterward  $x + 1$  mmol ( $x$  = number of alkoxy groups in the pyrazole) of borane-THF complex were added. The mixture was refluxed between 7 and 24 h. Then, the solvent was removed in the rotavapor and the residue was purified by silica chromatography with the eluent described below for each compound.

**1,3,5,7-Tetrakis(4'-*n*-decyloxyphenyl)pyrazabole (4C<sub>10</sub>).** Eluent: hexane/EtOAc (50/1). Yield: 34%. White solid. Anal. Calcd for C<sub>70</sub>H<sub>106</sub>B<sub>2</sub>N<sub>4</sub>O<sub>4</sub>: C, 77.18; H, 9.81; N, 5.14. Found: C, 77.24; H, 9.85; N, 5.11. IR (Nujol, NaCl):  $\nu$ (B-H) 2493, 2378,  $\nu$ (C=N, arC-C) 1612, 1578, 1496,  $\nu$ (C-O) 1253. <sup>1</sup>H NMR (CDCl<sub>3</sub>, 293 K):  $\delta$  0.87 (t,  $J$  = 6.7 Hz, 12H), 1.26-1.43 (m, 56H), 1.74-1.76 (m, 8H), 3.92 (t,  $J$  = 6.5 Hz, 8H), 6.27 (s, 2H), 6.85 (d,  $J$  = 8.6 Hz, 8H), 7.38 (d,  $J$  = 8.6 Hz, 8H). MS  $m/z$  (%): 1088 (100, [M<sup>+</sup>]), 571 (54), 533 (30).

**1,3,5,7-Tetrakis(3',4'-di-*n*-hexyloxyphenyl)pyrazabole (8C<sub>6</sub>-3,4).** Eluent: hexane/CH<sub>2</sub>Cl<sub>2</sub> (3/1). Yield: 29%. White solid. Anal. Calcd for C<sub>78</sub>H<sub>122</sub>B<sub>2</sub>N<sub>4</sub>O<sub>8</sub>: C, 74.04; H, 9.72; N, 4.43. Found: C, 73.87; H, 9.58; N, 4.45. IR (Nujol, NaCl):  $\nu$ (B-H) 2497, 2392,  $\nu$ (C=N, arC-C) 1608, 1585, 1502,  $\nu$ (C-O) 1242. <sup>1</sup>H NMR (CDCl<sub>3</sub>, 293K):  $\delta$  0.86-0.91 (m, 24H), 1.30-1.50 (m, 48H), 1.79-1.86 (m, 16H), 3.87 (t,  $J$  = 6.6 Hz, 8H), 3.98 (t,  $J$  = 6.6 Hz, 8H), 6.35 (s, 2H), 6.85 (d,  $J$  = 8.6 Hz, 4H), 7.03-7.06 (m, 8H). MS  $m/z$  (%): 1264 (100, [M<sup>+</sup>]), 660 (51).

(15) Strzelecka, H.; Jallabert, C.; Veber, M.; Malthe, J. *Mol. Cryst. Liq. Cryst.* **1988**, *156*, 347.

(16) Rubottom, G. M.; Kim, C. J. *Org. Chem.* **1983**, *48*, 1550.

(17) Ohta, K.; Ema, H.; Muroki, H.; Yamamoto, I.; Matsuzaki, K. *Mol. Cryst. Liq. Cryst.* **1987**, *147*, 61.



**1,3,5,7-Tetrakis(3',4'-di-*n*-decyloxyphenyl)pyrazabole (8C<sub>10</sub>-3,4).** Eluent: hexane/diethyl ether (20/1). Yield: 22%. White solid. Anal. Calcd for C<sub>110</sub>H<sub>186</sub>B<sub>2</sub>N<sub>4</sub>O<sub>8</sub>: C, 77.07; H, 10.94; N, 3.27. Found: C, 76.96; H, 10.71; N, 3.24. IR (Nujol, NaCl):  $\nu(\text{B-H})$  2498, 2388,  $\nu(\text{C=N, arC-C})$  1608, 1586, 1502,  $\nu(\text{C-O})$  1242. <sup>1</sup>H NMR (CDCl<sub>3</sub>, 293 K):  $\delta$  0.84–0.88 (m, 24H), 1.26–1.48 (m, 112H), 1.74–1.84 (m, 16H), 3.87 (t,  $J = 6.4$  Hz, 8H), 3.99 (t,  $J = 6.5$  Hz, 8H), 6.34 (s, 2H), 6.83 (d,  $J = 8.4$  Hz, 4H), 7.02 (s, 4H), 7.03 (d,  $J = 8.4$  Hz, 4H). MS  $m/z$  (%): 1713 (100, [M<sup>+</sup>]), 884 (85), 846 (80).

**1,3,5,7-Tetrakis(3',4'-di-*n*-(tetradecyloxy)phenyl)pyrazabole (8C<sub>14</sub>-3,4).** Eluent: hexane/CH<sub>2</sub>Cl<sub>2</sub> (1/4). Yield: 32%. White solid. Anal. Calcd for C<sub>142</sub>H<sub>248</sub>B<sub>2</sub>N<sub>4</sub>O<sub>8</sub>: C, 78.92; H, 11.57; N, 2.59. Found: C, 78.86; H, 11.98; N, 2.52. IR (Nujol, NaCl):  $\nu(\text{B-H})$  2497, 2378,  $\nu(\text{C=N, arC-C})$  1608, 1586, 1502,  $\nu(\text{C-O})$  1270. <sup>1</sup>H NMR (CDCl<sub>3</sub>, 293 K):  $\delta$  0.83–0.88 (m, 24H), 1.24–1.46 (m, 192H), 1.76–1.81 (m, 16H), 3.86 (t,  $J = 6.5$  Hz, 8H), 3.98 (t,  $J = 6.6$  Hz, 8H), 6.33 (s, 2H), 6.82 (d,  $J = 8.6$  Hz, 4H), 7.01 (s, 4H), 7.02 (d,  $J = 8.6$  Hz). MS  $m/z$  (%): 2160 (100, [M<sup>+</sup>]), 1070 (64).

**1,3,5,7-Tetrakis(3',5'-di-*n*-decyloxyphenyl)pyrazabole (8C<sub>10</sub>-3,5).** Eluent: hexane/CH<sub>2</sub>Cl<sub>2</sub> (5/2). Yield: 40%. White solid. Anal. Calcd for C<sub>110</sub>H<sub>186</sub>B<sub>2</sub>N<sub>4</sub>O<sub>8</sub>: C, 77.07; H, 10.94; N, 3.27. Found: C, 77.03; H, 10.98; N, 3.37. IR (Nujol, NaCl):  $\nu(\text{B-H})$  2475, 2400,  $\nu(\text{C=N, arC-C})$  1612, 1595, 1548,  $\nu(\text{C-O})$  1142. <sup>1</sup>H NMR (CDCl<sub>3</sub>, 293 K):  $\delta$  0.89 (t,  $J = 6.6$  Hz, 24H), 1.28–1.44 (m, 112H), 1.73–1.75 (m, 16H), 3.87 (t,  $J = 6.1$  Hz, 16H), 6.43 (s, 2H), 6.47 (s, 4H), 6.65 (s, 8H). MS  $m/z$  (%): 1713 (100, [M<sup>+</sup>]), 884 (91), 846 (82).

**1,5(7)-Bis(3',4',5'-tri-*n*-hexyloxyphenyl)-3,7(5)-bis(3'',4''-di-*n*-hexyloxyphenyl)pyrazabole (10C<sub>6</sub>).** Eluent: hexane/CH<sub>2</sub>Cl<sub>2</sub> (3/1). Yield: 58%. White solid. Anal. Calcd for C<sub>90</sub>H<sub>146</sub>B<sub>2</sub>N<sub>4</sub>O<sub>10</sub>: C, 73.75; H, 10.04; N, 3.82. Found: C, 73.83; H, 9.89; N, 3.80. IR (Nujol, NaCl):  $\nu(\text{B-H})$  2488, 2385,  $\nu(\text{C=N, arC-C})$  1607, 1584, 1495,  $\nu(\text{C-O})$  1241. <sup>1</sup>H NMR (CDCl<sub>3</sub>, 293 K):  $\delta$  0.83–0.90 (m, 30H), 1.24–1.45 (m, 60H), 1.70–1.81 (m, 20H), 3.80–4.00 (m, 20H), 6.35 (2s, 2H), 6.65 and 6.67 (2s, 4H), 6.83 (d,  $J = 7.9$  Hz, 2H), 7.03–7.06 (m, 4H). MS  $m/z$  (%): 1464 (35, [M<sup>+</sup>]), 722 (100).

**1,5(7)-Bis(3',4',5'-tri-*n*-decyloxyphenyl)-3,7(5)-bis(3'',4''-di-*n*-decyloxyphenyl)pyrazabole (10C<sub>10</sub>).** Eluent: hexane/CH<sub>2</sub>Cl<sub>2</sub> (5/2). Yield: 40%. White wax. Anal. Calcd for C<sub>130</sub>H<sub>226</sub>B<sub>2</sub>N<sub>4</sub>O<sub>10</sub>: C, 77.04; H, 11.24; N, 2.76. Found: C, 77.11; H, 11.35; N, 2.80. IR (Nujol, NaCl):  $\nu(\text{B-H})$  2490, 2384,  $\nu(\text{C=N, arC-C})$  1607, 1584, 1495,  $\nu(\text{C-O})$  1241. <sup>1</sup>H NMR (CDCl<sub>3</sub>, 293 K):  $\delta$  0.83–0.87 (m, 30H), 1.24–1.45 (m, 140H),

1.71–1.81 (m, 20H), 3.80–4.00 (m, 20H), 6.34 (2s, 2H), 6.62 and 6.64 (2s, 4H), 6.83 (d,  $J = 8.0$  Hz, 2H), 7.00–7.73 (m, 4H). MS  $m/z$  (%): 2025 (100, [M<sup>+</sup>]), 1040 (90).

**1,5(7)-Bis(3',4',5'-tri-*n*-(tetradecyloxy)phenyl)-3,7(5)-bis(3'',4''-di-*n*-(tetradecyloxy)phenyl)pyrazabole (10C<sub>14</sub>).** Eluent: hexane/CH<sub>2</sub>Cl<sub>2</sub> (5/2). Yield: 44%. White solid. Anal. Calcd for C<sub>170</sub>H<sub>306</sub>B<sub>2</sub>N<sub>4</sub>O<sub>10</sub>: C, 78.90; H, 11.92; N, 2.16. Found: C, 78.77; H, 11.69; N, 2.19. IR (Nujol, NaCl):  $\nu(\text{B-H})$  2484, 2383,  $\nu(\text{C=N, arC-C})$  1584, 1496,  $\nu(\text{C-O})$  1241. <sup>1</sup>H NMR (CDCl<sub>3</sub>, 293 K):  $\delta$  0.85–0.90 (m, 30H), 1.25–1.52 (m, 220H), 1.70–1.86 (m, 20H), 3.82–4.02 (m, 20H), 6.36 (2s, 2H), 6.66 and 6.68 (2s, 4H), 6.85 (d,  $J = 8.2$  Hz, 1H), 7.02–7.08 (m, 4H). MS  $m/z$  (%): 2587 (100, [M<sup>+</sup>]), 1320 (87).

**1,5(7)-Bis(2',3',4'-tri-*n*-decyloxyphenyl)-3,7(5)-bis(3'',4'',5''-tri-*n*-decyloxyphenyl)pyrazabole (12C<sub>10</sub>unsym).** Eluent: hexane/CH<sub>2</sub>Cl<sub>2</sub> (5/1). Yield: 27%. White wax. Anal. Calcd for C<sub>150</sub>H<sub>266</sub>B<sub>2</sub>N<sub>4</sub>O<sub>12</sub>: C, 77.01; H, 11.46; N, 2.39. Found: C, 77.33; H, 11.26; N, 2.32. IR (Nujol, NaCl):  $\nu(\text{B-H})$  2473, 2401,  $\nu(\text{C=N, arC-C})$  1601, 1584, 1487,  $\nu(\text{C-O})$  1240. <sup>1</sup>H NMR (CDCl<sub>3</sub>, 293 K):  $\delta$  0.77–0.85 (m, 36H), 1.24–1.50 (m, 168H), 1.71–1.81 (m, 24H), 3.74–3.95 (m, 24H), 6.39 and 6.41 (2s, 2H), 6.57 (d,  $J = 8.8$  Hz, 2H), 6.65 y 6.69 (2s, 4H), 6.92 and 6.99 (2d,  $J = 8.8$  Hz, 2H). MS  $m/z$  (%): 2339 (100, [M<sup>+</sup>]), 1159 (25).

**1,3,5,7-Tetrakis(3'',4'',5''-tri-*n*-decyloxyphenyl)pyrazabole 12C<sub>10</sub>sym.** Eluent: hexane/CH<sub>2</sub>Cl<sub>2</sub> (5/1). Yield: 24%. White solid. Anal. Calcd for C<sub>150</sub>H<sub>266</sub>B<sub>2</sub>N<sub>4</sub>O<sub>12</sub>: C, 77.01; H, 11.46; N, 2.39. Found: C, 77.00; H, 11.34; N, 2.34. IR (Nujol, NaCl):  $\nu(\text{B-H})$  2508, 2410, 2360,  $\nu(\text{C=N, arC-C})$  1582, 1550, 1516, 1491,  $\nu(\text{C-O})$  1238. <sup>1</sup>H NMR (CDCl<sub>3</sub>, 293 K):  $\delta$  0.83–0.88 (m, 36H), 1.25–1.47 (m, 168H), 1.72–1.77 (m, 24H), 3.85 (t,  $J = 6.2$  Hz, 16H), 3.95 (t,  $J = 6.5$  Hz, 8H), 6.35 (s, 2H), 6.66 (s, 8H). MS  $m/z$  (%): 2339 (100, [M<sup>+</sup>]), 1158 (42).

**Acknowledgment.** We thank the CICYT project MAT97-0986-C02-01 from the Ministerio de Educación y Ciencia (Spain) for financial support and the CONSI+D department of the Diputación General de Aragón for a research studentship to R. G.

**Supporting Information Available:** An X-ray crystallographic file, in CIF format, for compound 4C<sub>1</sub>. This material is available free of charge via the Internet at <http://pubs.acs.org>.

CM991120C